Synthesis of Coupled-Resonators Group-Delay Equalizers

Heng-Tung Hsu, *Student Member, IEEE*, Hui-Wen Yao, *Senior Member, IEEE*, Kawthar A. Zaki, *Fellow, IEEE*, and Ali E. Atia, *Fellow, IEEE*

***Abstract*—A systematic synthesis and design procedure for coupled-resonators cavity group-delay equalizers is presented. The procedure consists of solving the approximation problem by optimization and performing cascade synthesis. The error function for the optimization is computed from the given filter's group delay and the zeros and poles of the input impedance of the equalizer. Convergence of the optimization is fast and insensitive to the initial guess even when the number of resonators is large. Two examples, together with experimental results, are presented; comparisons between the externally equalized and self-equalized filters are made. The effect of the isolation of the cascading devices (circulator or 3-dB hybrid) on the ripple of the final group-delay response is also extensively investigated. The good agreement between the theoretical simulation and the experimental results demonstrates the powerful nature and effectiveness of the proposed design procedure.**

***Index Terms*—Delay equalizer, optimization, resonators.**

I. Introduction

MICROWAVE bandpass networks, together with equalization circuitry, are essential components in modern communication systems such as satellite communication systems. The concept of external group-delay equalization has been applied extensively [1]–[4] and comparisons are made on the overall responses with the self-equalized filters. In general, self-equalized linear phase filters are smaller structures, require no cascading devices (circulator or 3-dB hybrids), but are relatively complex and difficult to design and tune. Also, the maximum number of equalization poles is often limited by the filter structures (for example, an eight-pole quasi-elliptic function filter with two transmission zeros can only afford one equalization pole). On the other hand, externally equalized structures are nearly independent of the associated filter, which simplifies the design and tuning process and demonstrates much more flexibility. Nevertheless, the self-equalized structures show better performance consistency over temperature variation, which is a key advantage over the externally equalized one for satellite applications.

Conventional realizations of group-delay equalizers for externally equalized structures are mostly limited to all-pass C-sections (all-pass first-order) and all-pass D-section (all-pass second-order) networks cascaded with circulators or 3-dB hybrids. Graphical methods have been used to determine the suitable locations of zeros of an equalizer followed by Richards' synthesis procedure to complete the design [5], [6]. This approach works well when the amount of equalization required is small. When a larger amount of equalization is needed, several C- or D-section equalizers may be required in cascade, which makes the design of such equalizers difficult.

A design method for equalizers with multiple coupled cavities was first presented in 1982 [7]. Direct network optimization has been used in [7], where the coupling matrix elements are the optimization variables and the difference between the group-delay response of the equalizer and frequency specification mask is the basis for the objective error function. Optimization routines or available commercial software packages may be used to solve for all the optimization variables by minimizing the objective error function over the frequency band of interest. The design method proposed in [7] showed the two major advantages over the conventional approach, i.e., a single equalizer with multiple poles is able to perform a larger degree of equalization that provides a considerable hardware weight reduction over the conventional approach of using several cascaded C- or D-sections and equalizer parameters are directly generated through the optimization process, which eliminates the synthesis step, making the design procedure easy and straightforward.

However, the approach proposed in [7] is usually inefficient and often results in nonoptimum (local minimum) solutions. Moreover, the convergence of numerically minimizing the objective error function will depend strongly on the initial guess of the equalizer parameters (coupling matrix elements), especially when the number of cavities is large. In this paper, a systematic design procedure is presented. This new and powerful design procedure basically consists of two separate steps, i.e., solving the approximation problem through numerical optimization and solving the synthesis problem. The objective error function used for solving the approximation problem is based on evaluating the group-delay response using the zeros and poles of the input impedance function of the structure. Convergence of the optimization of the proposed design method is fast and nearly independent of the initial guess of zeros and poles locations even when the number of the cavities is large. Once the locations of zeros and poles are determined, a synthesis procedure is then carried out to complete the design.

In Section II, the problem statement and detailed circuit analysis for the approximation problem are presented. A straightforward synthesis procedure together with some numerical considerations to improve the accuracy for the synthesis problem are

Manuscript received August 8, 2001.

H.-T. Hsu and K. A. Zaki are with the Department of Electrical and Computer Engineering, University of Maryland at College Park, College Park, MD 20742 USA.

H.-W. Yao and A. E. Atia are with the Orbital Sciences Corporation, Dulles, VA 20166 USA.

Publisher Item Identifier 10.1109/TMTT.2002.801344.

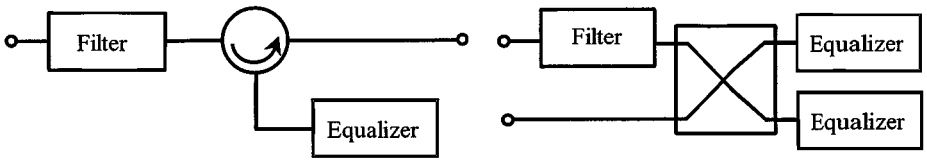

Fig. 1. Schematic drawings of: (a) circulator-coupled and (b) 3-dB hybrid branch coupler coupled filter–equalizer network.

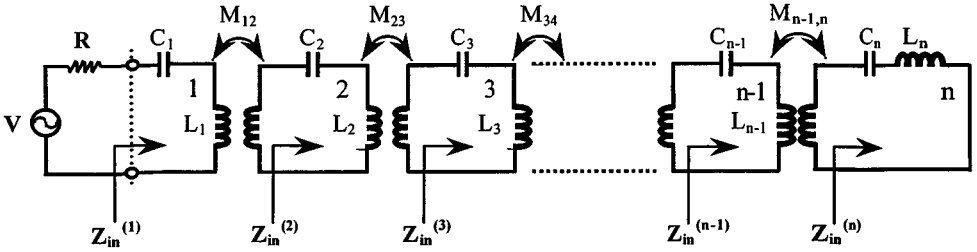

Fig. 2. Equivalent-circuit representation of an n-cavity narrow-band equalizer.

addressed in Section III. Two numerical examples with experimental results of an eight-pole elliptic function filter equalized by a three-pole equalizer are included in Section IV. Comparisons between a 12-pole self-equalized filter and an eight-pole externally equalized (by a three-pole equalizer) one are made and summarized. The effect of the isolation of the cascading devices (circulator or 3-dB hybrid) on the ripple of the final group-delay response is also investigated. Good agreement observed between the theoretical simulation and the experimental results shows the powerful nature and effectiveness of the proposed design method.

II. Approximation Problem

Consider a circulator coupled filter–equalizer network, as shown in Fig. 1(a), or hybrid coupled network, as shown in Fig. 1(b). Since the total group delay of the network is the sum of the group delay of the filter and the reflection delay of the equalizer, ideally, the delay characteristics of the equalizer should be the inverse of the filter's to compensate for the steep change at the edges of the band. The delay of the equalizer is the delay characteristic of the reflection coefficient of a short-circuited coupled-resonators filter [8]–[10].

Fig. 2 shows the equivalent lumped-circuit representation for a short-circuited coupled-resonators narrow-band equalizer. Although this equivalent circuit is accurate only over a narrow bandwidth (<20%), it is usually sufficient in most applications where a large amount of equalization is only required over a narrow bandwidth. The input impedance of the equalizer can be obtained as [11]

$$Z_{\text{in}}^{(i)} = j\,\frac{Z_{oi}}{\omega\omega_{oi}}\,\frac{P_i(\omega^2)}{Q_i(\omega^2)}, \qquad i = 1, \ldots, n. \tag{1}$$

$P_1(\omega^2)$ and $Q_1(\omega^2)$ are monic polynomials of order n and $(n-1)$, respectively, $\omega_{o1} = 1/\sqrt{L_1C_1}$ is the resonant frequency of the first resonator, and $Z_{o1} = \sqrt{L_1/C_1}$ is the characteristic impedance of the first resonator. The input reflection coefficient of the equalizer can be readily expressed as

$$\rho_{\text{in}}(\omega) = \frac{Z_{\text{in}}^{(1)}(\omega) - R}{Z_{\text{in}}^{(1)}(\omega) + R} = |\rho_{\text{in}}(\omega)|e^{j\phi(\omega)} \tag{2}$$

$$\phi(\omega) = -2\tan^{-1}\left[\frac{Z_{o1}P_1(\omega^2)}{\omega\omega_{o1}RQ_1(\omega^2)}\right]. \tag{3}$$

The group delay of the equalizer, by definition, is the negative derivative of $\phi(\omega)$ with respect to ω. Noting the fact that the input impedance (1) is purely reactive for lossless networks, the group delay of the equalizer can then be easily derived as [11]

$$\tau_E(\omega) = -\frac{d\phi(\omega)}{d\omega} = \frac{2\omega_{o1}\,\dfrac{R}{Z_{o1}}\left[\omega\left(\dfrac{P_1'}{P_1} - \dfrac{Q_1'}{Q_1}\right) - 1\right]}{\left(\dfrac{P_1}{Q_1}\right) + \left(\dfrac{\omega\omega_{o1}R}{Z_{o1}}\right)^2\left(\dfrac{Q_1}{P_1}\right)} \tag{4}$$

where P_1' and Q_1' denote the first derivatives of P_1 and Q_1 with respect to ω, respectively. When the network shown in Fig. 2 is near the optimum approximation to the requirement, $P_1(\omega^2)$ and $Q_1(\omega^2)$ can be expressed as [8], [10]

$$P_1\left(\omega^2\right) = \prod_{i=1}^{n}\left(\omega^2 - \omega_{zi}^2\right) \tag{5a}$$

$$Q_1\left(\omega^2\right) = \prod_{j=1}^{n-1}\left(\omega^2 - \omega_{pj}^2\right). \tag{5b}$$

In the above expressions, ω_{zi} $(i = 1, 2, \ldots, n)$ and ω_{pj} $(j = 1, 2, \ldots, n-1)$ are zeros of P_1 and Q_1, corresponding to the zeros and poles of the input impedance function, respectively.

The approximation problem can be stated as follows. Given a certain requirement on the group delay (frequency specification mask) to be met by the proposed network, determine the locations of the zeros and poles of the input impedance function of the equalizer that realize the desired group-delay characteristic. The approximation problem is solved numerically through optimization. The optimization procedure starts by an initial guess

for the locations of zeros and poles. A simple initial guess will be taking the initial placement of the zeros and poles to be alternating and equally distributed over the desired bandwidth. The objective error function is defined as

$$\begin{aligned}&\mathrm{Errf}(\overline{x})\\&\quad=\sum_i\left|\tau_F(\omega_i)+\tau_E(\omega_i)-\tau_{\min}-T_{\mathrm{mask}}(\omega_i)\right|^2\\&\overline{x}=\left(\omega_{z1},\omega_{z2},\ldots,\omega_{zn},\omega_{p1},\omega_{p2},\ldots,\omega_{p,n-1},R/Z_{o1}\right)\\&i\in\left\{\tau_F(\omega_i)+\tau_E(\omega_i)-\tau_{\min}-T_{\mathrm{mask}}(\omega_i)>0\right\}\end{aligned}\tag{6}$$

with τ_F and τ_E being the group delay of the filter and equalizer; $\tau_{\min}$ is the minimum of the total group delay (constant), and T_{mask} is the required frequency specification mask for group delay. In the above expression, τ_E and $\tau_{\min}$ are evaluated from the current placement of the zeros and poles. A standard constrained gradient search algorithm is used to minimize the objective error function since the locations of the zeros and poles of the reactance function are known to be interlaced in the vicinity of the passband of the filter network, i.e., $\omega_{z1}<\omega_{p1}<\omega_{z2}<\omega_{p2}<\cdots<\omega_{z,n-1}<\omega_{p,n-1}<\omega_{z,n}$.

Convergence of the minimization is fast due to the constrained nature among the optimization variables (the zeros and poles of the input impedance of the equalizer). On the contrary, however, the difficulty of the proposed approach in [7] (where the coupling matrix elements are primarily the optimization variables) mainly comes form the lack of any known relationship among them, especially when the number of cavities is large. In most cases, the required frequency specification mask for group delay (T_{mask}) will be symmetric with respect to center frequency. In such cases, the speed of convergence can be dramatically improved since only half the number of optimization variables is necessary for optimization.

III. Synthesis Prodedure

After solving the approximation problem, the exact locations of the zeros and poles that realize the required group-delay characteristic of the network are known. To complete the design, a synthesis procedure is adopted to extract the equalizer parameters from the knowledge of the locations of zeros and poles of the network.

Using the same notations as defined in Fig. 2, the input impedance at loop i can be obtained as

$$Z_{\mathrm{in}}^{(i)}(\omega)=j\,\frac{Z_{oi}}{\omega\omega_{oi}}\,\frac{P_i(\omega^2)}{Q_i(\omega^2)},\qquad i=1,2,\ldots,n\tag{7}$$

where $\omega_{oi}=1/\sqrt{L_iC_i}$ is the resonant frequency of resonator i and $Z_{oi}=\sqrt{L_i/C_i}$ is the characteristic impedance of the ith resonator. The monic polynomials $P_i(\omega^2)$ and $Q_i(\omega^2)$ are expressed as [10]

$$P_i(\omega^2)=\sum_{t=0}^{n-i+1}c_t^{(i)}(\omega^2)^t=\prod_{t=1}^{n-i+1}\left(\omega^2-\omega_{zt}^{(i)^2}\right),\qquad i=1,2,\ldots,n\tag{8}$$

$$Q_i(\omega^2)=\sum_{q=0}^{n-i}d_q^{(i)}(\omega^2)^q=\prod_{q=1}^{n-i}\left(\omega^2-\omega_{pq}^{(i)^2}\right),\qquad i=1,2,\ldots,n.\tag{9}$$

Since the circuit model of Fig. 2 is an accurate representation over a narrow bandwidth, as discussed previously, the coupling coefficients between two adjacent resonators $k_{i,i+1}$ can be modeled as frequency-independent reactance and can be defined as

$$k_{i,i+1}^2=\frac{M_{i,i+1}^2}{Z_{oi}Z_{oi+1}},\qquad i=1,2,\ldots,n-1.\tag{10}$$

The coupling bandwidth $m_{i,i+1}$ is then defined as

$$m_{i,i+1}^2=\omega_{oi}\omega_{oi+1}\,\frac{M_{i,i+1}^2}{Z_{oi}Z_{oi+1}},\qquad i=1,2,\ldots,n-1\tag{11}$$

and is the coupling coefficient in frequency unit. The following recursive relations can be derived from basic circuit theory:

$$P_{i+1}(\omega^2)=Q_i(\omega^2),\qquad i=1,2,\ldots,n-1\tag{12}$$

$$m_{i,i+1}^2\omega^2Q_{i+1}(\omega^2)=(\omega^2-\omega_{0i}^2)P_{i+1}(\omega^2)-P_i(\omega^2),\qquad i=1,2,\ldots,n-1\tag{13}$$

$$\omega_{0i}^2=\frac{\prod_{t=1}^{n-i+1}\omega_{zt}^{(i)^2}}{\prod_{q=1}^{n-i}\omega_{pq}^{(i)^2}}=-\frac{c_0^{(i)}}{d_0^{(i)}},\qquad i=1,2,\ldots,n\tag{14}$$

$$\begin{aligned}m_{i,i+1}^2&=\sum_{t=1}^{n-i+1}\omega_{zt}^{(i)^2}-\sum_{q=1}^{n-1}\omega_{pq}^{(i)^2}-\omega_{0i}^2\\&=d_{n-i-1}^{(i)}-c_{n-i}^{(i)}-\omega_{0i}^2,\\&\qquad i=1,2,\ldots,n-1.\end{aligned}\tag{15}$$

Equations (14) and (15) give explicit relations between the equalizer parameters and the locations of zeros and poles. In most cases, the equalizer parameters can be effectively synthesized from known locations of the zeros and poles using the recursive relations given in (12)–(15). However, in some cases when the bandwidth of the equalizer is small or the number of the cavities is large, the numerical accuracy may become quite an issue. The cancellation of the coefficients of the highest order terms in (13) is not guaranteed in the above cases. To further improve the numerical accuracy, the following transformation of variable is introduced:

$$\lambda=\left(\frac{f}{f_o}-\frac{f_o}{f}\right)\cdot\frac{f_o}{\mathrm{BW}}\tag{16}$$

where f_o and BW are the center frequency and bandwidth of the equalizer, respectively.

The input impedance at loop i of the circuit can then be derived in the transformed domain as

$$Z_{\mathrm{in}}^{(i)}(\lambda)=jZ_{oi}\,\frac{P_i(\lambda)}{Q_i(\lambda)},\qquad i=1,2,\ldots,n\tag{17}$$

with the monic polynomials $P_i(\lambda)$ and $Q_i(\lambda)$ expressed as

$$P_i(\lambda) = \sum_{t=0}^{n-i+1} c_t^{(i)}(\lambda)^t = \prod_{t=1}^{n-i+1}\left(\lambda - \lambda_{zt}^{(i)}\right), \quad i = 1, 2, \ldots, n \tag{18}$$

$$Q_i(\lambda) = \sum_{q=0}^{n-i} d_q^{(i)}(\lambda)^q = \prod_{q=1}^{n-i}\left(\lambda - \lambda_{pq}^{(i)}\right), \quad i = 1, 2, \ldots, n. \tag{19}$$

Finally, the following recursive relations can be obtained:

$$P_{i+1}(\lambda) = Q_i(\lambda), \qquad i = 1, 2, \ldots, n-1 \tag{20}$$

$$\left(\lambda + c_{n-i}^{(i)} - d_{n-i-1}^{(i)}\right) P_{i+1}(\lambda) - P_i(\lambda) = k_{i,i+1}^2 Q_{i+1}(\lambda), \qquad i = 1, 2, \ldots, n-1 \tag{21}$$

$$\omega_{oi}^2 = \omega_o\left(1 - \frac{c_{n-i}^{(i)} - d_{n-i-1}^{(i)}}{2}\right), \qquad i = 1, 2, \ldots, n \tag{22}$$

$$k_{i,i+1}^2 = \left(c_{n-i}^{(i)} - d_{n-i-1}^{(i)}\right) d_{n-i-1}^{(i)} + d_{n-i-2}^{(i)} - c_{n-i-1}^{(i)}, \quad i = 1, 2, \ldots, n-1. \tag{23}$$

Note that $d_{-1}^{(i)} = 0$ in both (22) and (23).

IV. Design Examples

A computer program has been developed to solve the approximation problem through optimization and perform the synthesis of the equalizer as described. Many design examples have been run to verify and test the program. Convergence of the optimization is fast and, in all cases, tested is nearly independent of the initial placement of the zeros and poles. In contrast, direct network optimization using an error function based on the difference between the mask and response was slow, often did not converge to any acceptable solution, and in all cases, required an initial guess as to whose response was close to the desired one in order to converge, especially when the number of cavities was large.

As an application, two equalizers are designed according to the method described in the previous sections. In the first design (Design A), the filter to be equalized is a 16-pole elliptic function filter with a bandwidth of 20 MHz centered at 2 GHz. Fig. 3(a) shows the typical in-band insertion loss and group-delay response of the filter. The required group-delay variation after equalization is 65 ns over 96.2% of filter's passband. An equalizer with 12 poles is designed to equalize the filter. The locations of the zeros and poles after solving the approximation problem together with the synthesized equalizer parameters are listed in Table I. Since we have many poles $(n = 12)$ over a very narrow bandwidth (1.04%) in this case, working in the transformed domain (λ domain) is necessary to achieve the required accuracy. Fig. 3(b) shows the simulated final response (in-band insertion loss and group delay) of both the filter and equalizer cascaded through an ideal circulator.

The second design (Design B) involves an eight-pole elliptic function filer to be equalized so that its group delay lies within

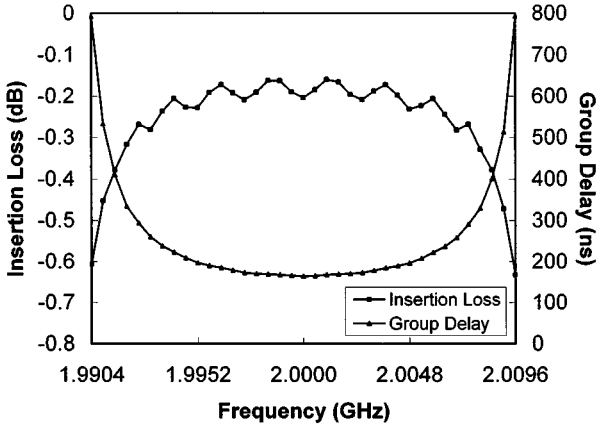

(a)

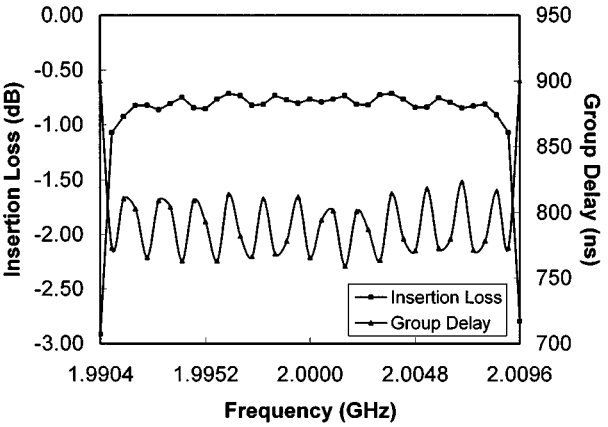

(b)

Fig. 3. (a) Typical in-band responses (insertion loss and group delay) of the 16-pole elliptic function filter used in Design A. (b) Simulated final response of the in-band insertion loss and group delay of the filter and equalizer cascaded through an ideal circulator. The specified group-delay variation is 65 ns over 96.2% of filter's bandwidth. In both (a) and (b), the unloaded Q is set to be 55 000 (superconductor).

TABLE I
Detail Parameters for the Equalizer in Design A

Locations of Zeros and Poles After Solving the Approximation Problem		Synthesized Equalizer Parameters (Normalized Coupling Matrix)	
f_{zero} (GHz)	f_{pole} (GHz)		
1.9989	1.9911	R_{in}	1.2229
1.9922	1.9932	$M_{1,2}$	0.8827
1.9941	1.9950	$M_{2,3}$	0.5734
1.9958	1.9967	$M_{3,4}$	0.5218
1.9975	1.9983	$M_{4,5}$	0.4685
1.9992	2.0000	$M_{5,6}$	0.4447
2.0008	2.0017	$M_{6,7}$	0.4242
2.0025	2.0033	$M_{7,8}$	0.3796
2.0041	2.0051	$M_{8,9}$	0.3492
2.0059	2.0068	$M_{9,10}$	0.3194
2.0078	2.0089	$M_{10,11}$	0.2602
2.0111		$M_{11,12}$	0.1829

the ranges defined in Table II by an equalizer with three poles. The filter has a bandwidth of 40 MHz and center frequency of 4 GHz. The requirement for overall equalized group delay is given through a frequency specification mask shown in Fig. 4. The same design method as in Design A is applied. In both designs (i.e., Designs A and B), the initial placement of the zeros and poles is taken to be equally distributed in the vicinity of the

TABLE II
GROUP-DELAY SPECIFICATION MASK FOR DESIGN B

Shift from Center Freq. (MHz)	Group Delay (nsec)
±4	0.8
±8	1.8
±12	4.5
±16	9.0
±18	19.5

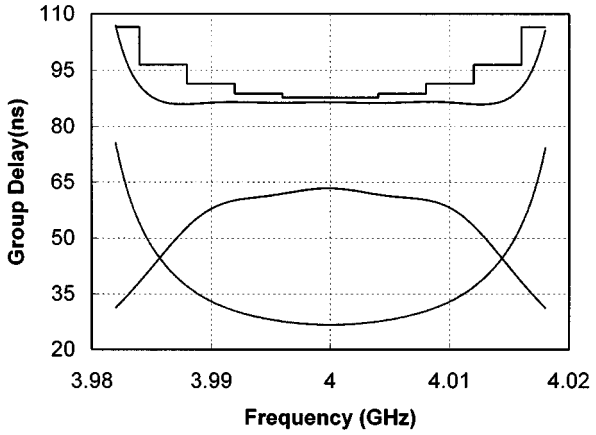

Fig. 4. Group-delay responses after optimization for Design B. The four curves shown in the plot are, from the top to the bottom, the frequency specification mask, final group delay of the filter and equalizer cascaded by an ideal circulator, group delay of the equalizer itself, and group delay of the filter only.

TABLE III
DETAIL PARAMETERS FOR THE EQUALIZER IN DESIGN B

Locations of Zeros and Poles After Solving the Approximation Problem		Synthesized Equalizer Parameters (Normalized Coupling Matrix)	
f_{zero} (GHz)	f_{pole} (GHz)		
3.98029	3.99180	R_{in}	1.3738
4.00024	4.00868	$M_{1,2}$	0.8402
4.02028		$M_{2,3}$	0.3911

bandwidth of the network. Only half the number of optimization variables is used to speed up the convergence of optimization since the frequency specification masks for the group delay are symmetric in both cases. Table III summarizes the detailed parameters of the equalizer for Design B and Fig. 4 shows the simulated results.

For comparison, 12-pole self-equalized filters with different number of equalization poles are designed according to the parameters specified in Design B. The maximum number of equalization poles can be afforded by the structure is three since two transmission zeros are necessary for the selectivity purpose. Fig. 5(a) and (b) shows the comparisons for the normalized group delay and in-band insertion loss. All the curves are generated using the same equal-ripple bandwidth (40 MHz). Fig. 6(a) and (b) shows the same comparisons with curves generated according to the same "transmission mask" as the eight-pole externally equalized one. In this case, the bandwidth of the 12-pole self-equalized filters is larger (44 MHz) than the eight-pole externally equalized one (40 MHz).

In all the figures, the externally equalized structure clearly shows larger bandwidth of equalization with comparable insertion loss. Moreover, the externally equalized structure tends to

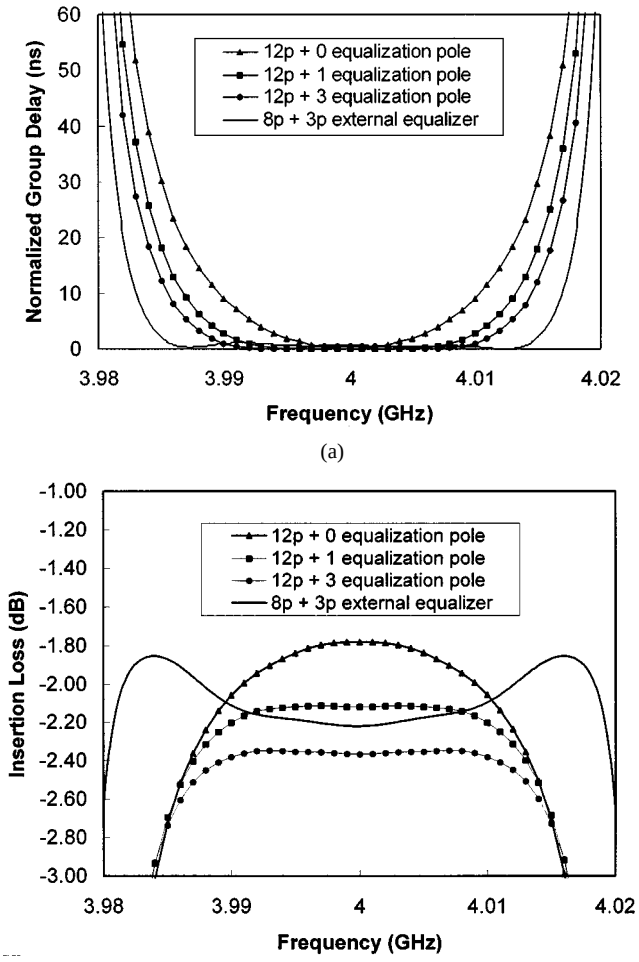

Fig. 5. Comparisons of: (a) normalized group delay and (b) insertion loss of the self-equalized and externally equalized filters. All the curves are generated using the same equal-ripple bandwidth.

have flatter in-band transmission response, which is also important for many communication systems applications. The required bandwidth of equalization can only be achieved by an externally equalized structure in this case, as is evidenced by the enlarged plot shown in Fig. 7. Increasing the number of poles for the self-equalized structure does not significantly improve the performance, but results in tremendous increase in the complexity of design and tuning (point of diminishing return).

To verify the accuracy of the design procedure, the equalizer for Design B together with the eight-pole elliptic function filter are built and tested. Both filter and equalizer are realized as combline resonators. Fig. 8(a) shows the measured transmission and reflection responses, while Fig. 8(b) shows the measured in-band responses (insertion loss and group delay) of the filter itself. A commercially available circulator with 28-dB isolation (measured) is used as the cascading device to cascade the filter and the equalizer. Fig. 9 shows the measured and simulated group delay of the overall network including the eight-pole filter, three-pole equalizer, and 28-dB isolation circulator. The simulated response of using an ideal circulator with infinite isolation as the cascading device is also included in the plot for comparison. It can be easily concluded from the figure that the isolation of the cascading device will have a pronounced effect

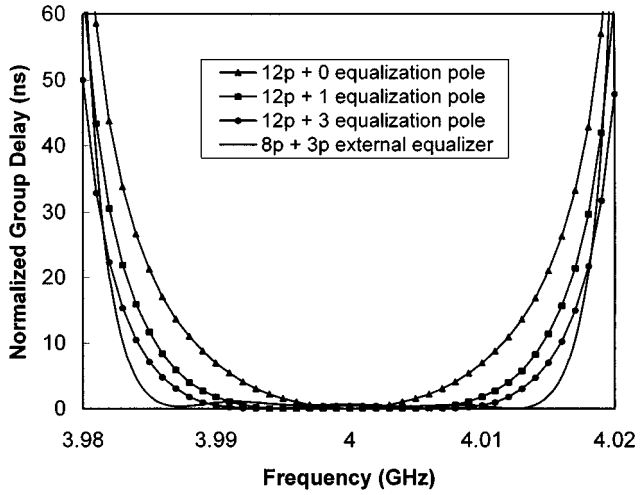

(a)

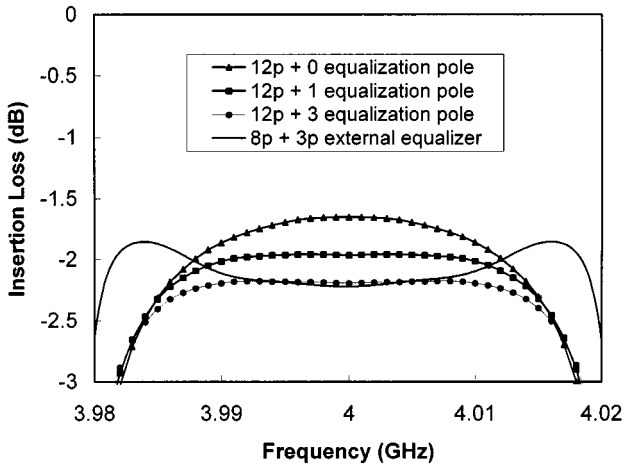

(b)

Fig. 6. Comparisons of: (a) normalized group delay and (b) insertion loss of the self-equalized and externally equalized filters. All the curves are generated using the same transmission mask.

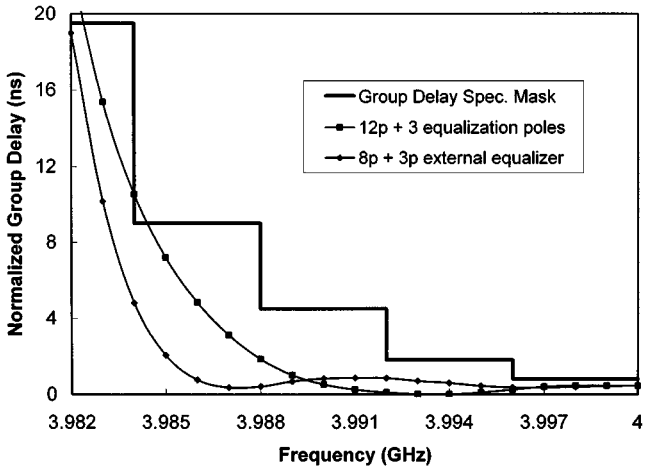

Fig. 7. Enlarged plot from Fig. 6(a) comparing the normalized group delay of the self-equalized and externally equalized filters. The self-equalized structure misses the group-delay specification, while the externally equalized one has a larger margin at the band edge. Only the left-hand-side half is plotted here since the response is symmetric.

on the ripple of the final group-delay response. Good agreement between the simulated result and measurement is observed.

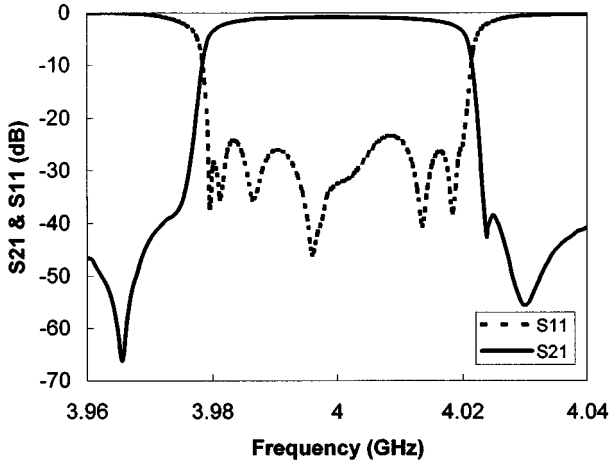

(a)

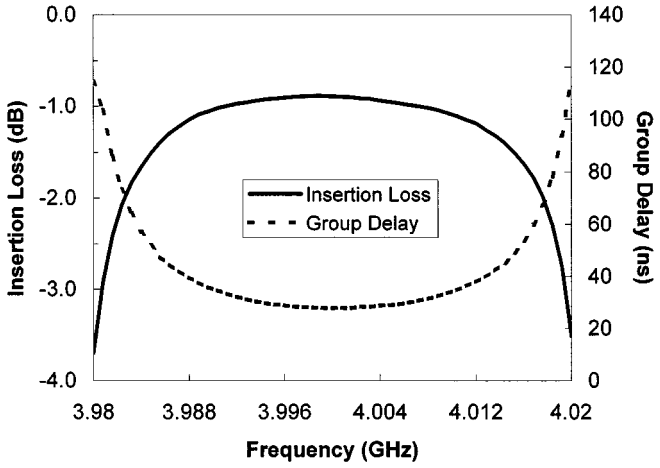

(b)

Fig. 8. Measured filter response of the eight-pole elliptic function filter in Design B realized in a combline structure. (a) Transmission and reflection. (b) In-band insertion loss and group delay. The unloaded Q of the filter is 3500.

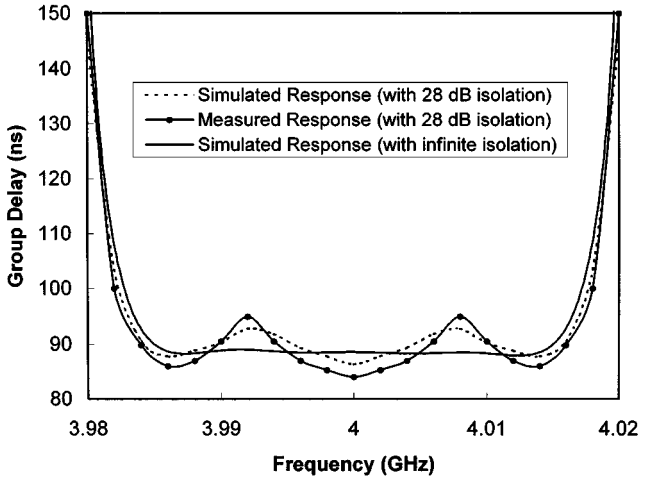

Fig. 9. Measured and simulated group-delay response of the circulator coupled filter–equalizer network for Design B. The circulator used has a measured isolation of 28 dB. The simulated response of the same network using an ideal circulator (with infinite isolation) is also included for comparison.

It is not feasible to take the finite isolation of the circulator into account in the optimization process. For the structure shown in Fig. 10(a), where a circulator with finite isolation $(\varepsilon, \varepsilon \ll 1)$

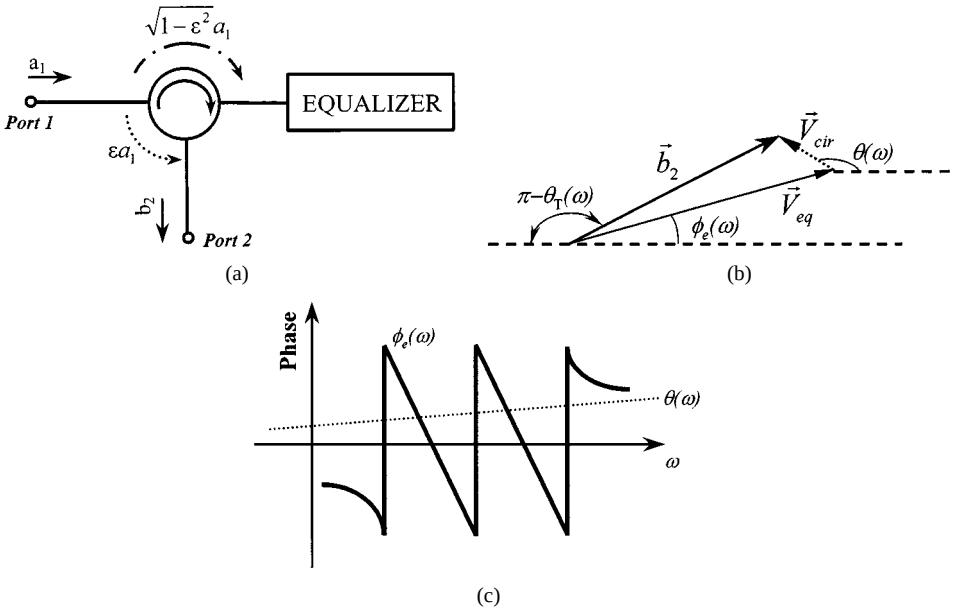

Fig. 10. (a) Illustration of the signal paths for circulator–equalizer network with finite isolation on the circulator. (b) Vector diagram representation of (a). (c) Typical phase response as functions of frequency for a three-pole equalizer and the circulator.

is used to cascade the filter and the equalizer, the output at port 2 can be represented as

$$b_2 = \sqrt{1-\varepsilon^2}\,a_1 e^{j\phi_e(\omega)} + \varepsilon a_1 e^{j\theta(\omega)} = \overrightarrow{V_{\text{eq}}} + \overrightarrow{V_{\text{cir}}} \qquad (24)$$

where $\phi_e(\omega)$ is the phase response of the input reflection coefficient of the equalizer and $\theta(\omega)$ is the phase response between the isolated and input ports of the circulator.

The phasor diagram representation for (24) is shown in Fig. 10(b). The overall phase response $\theta_T(\omega)$ between ports 2 and 1 will be added to the filter's phase response. Since the change rates of $\phi_e(\omega)$ and $\theta(\omega)$ with respect to frequency are quite different (usually $\phi_e(\omega)$ varies faster than $\theta(\omega)$, as shown in Fig. 10(c) for the case of a three-pole equalizer), synchronization of the two phases at port 2 is impossible. Namely, it is not possible for the same equalizer to "frequency-selectively" produce different component that cancels out the effect introduced by $\overrightarrow{V_{\text{cir}}}$. To further investigate the effect of the finite isolation, (24) can be rewritten as [refer to Fig. 10(a)]

$$S_{21}(\omega) = \frac{b_2}{a_1} = \sqrt{1-\varepsilon^2}\,e^{j\phi_e(\omega)} + \varepsilon e^{j\theta(\omega)} = |S_{21}(\omega)|e^{j\theta_T(\omega)}. \qquad (25)$$

The group delay of the corresponding network (the circulator and the equalizer), by definition, is

$$\begin{aligned}\tau(\omega) &= -\frac{d\theta_T(\omega)}{d\omega} \\ &= -\text{Im}\left\{\frac{d[\ln S_{21}(\omega)]}{d\omega}\right\} \\ &= -\frac{d\theta(\omega)}{d\omega} - \frac{1+\cos\phi_a(\omega)\cdot k}{1+2\cdot k\cdot\cos\phi_a(\omega)+k^2}\cdot\frac{d\phi_a(\omega)}{d\omega}\end{aligned} \qquad (26)$$

with

$$k = \frac{\varepsilon}{\sqrt{1-\varepsilon^2}} \text{ and } \phi_a(\omega) = \left[\phi_e(\omega) - \theta(\omega)\right].$$

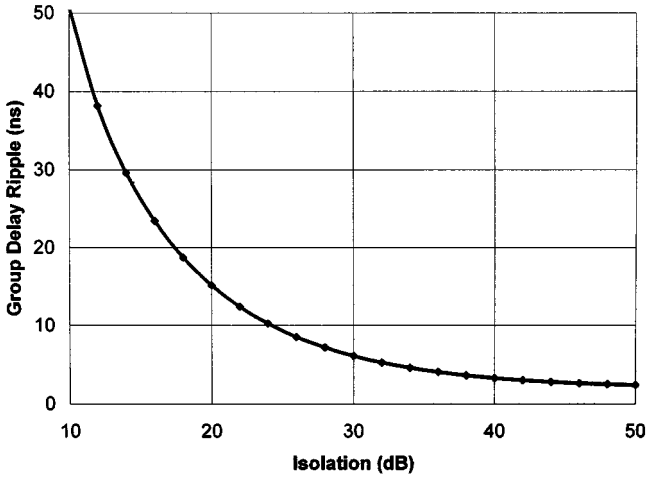

Fig. 11. Upper bound of the ripple of the group delay of the circulator–equalizer network versus the isolation of the circulator. The group delay of the equalizer at the center frequency is used to generate the plot.

Noting that $\theta(\omega)$ is a slow varying function of ω and $\tau_E(\omega) = -d\phi_e(\omega)/d\omega$ (the group delay of the equalizer), (26) can then be expressed as

$$\tau(\omega) = \tau_E(\omega)\,\frac{1+k\cdot\cos\left[\phi_e(\omega)-\theta(\omega)\right]}{1+2\cdot k\cdot\cos\left[\phi_e(\omega)-\theta(\omega)\right]+k^2}. \qquad (27)$$

The extremes (minimum or maximum) of the above expression will occur when $\phi_e(\omega) = \theta(\omega) \pm \pi, 2\pi, 3\pi, \ldots$ and the values of the extremes can be derived as

$$\begin{aligned}\tau_{\max}(\omega) &= \tau_E(\omega)\,\frac{1}{1-k} \\ \tau_{\min}(\omega) &= \tau_E(\omega)\,\frac{1}{1+k}.\end{aligned} \qquad (28)$$

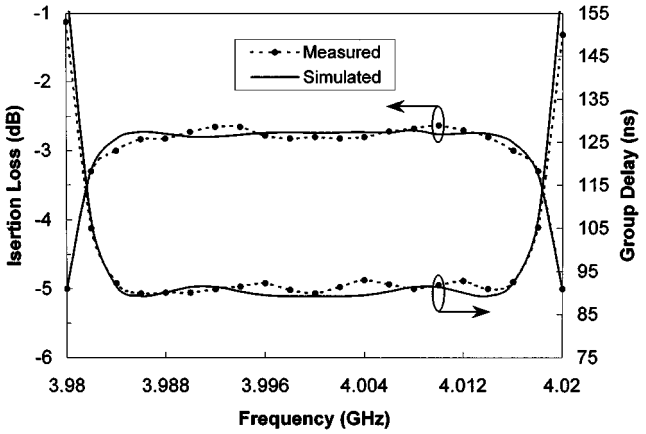

Fig. 12. Measured and simulated results of the in-band characteristics (both insertion loss and group delay) for the 3-dB hybrid coupled filter–equalizer network.

Finally, the explicit expression for the ripple of group delay as a function of ε can be derived as

$$\Delta\tau_{\text{peak-to-peak}} = \tau_E(\omega)\,\frac{2\varepsilon\sqrt{1-\varepsilon^2}}{1-2\varepsilon^2}. \tag{29}$$

Fig. 11 shows the plot of the upper bound ripple of the group delay versus the isolation of the circulator for the case of Design B. The value at the center frequency $\tau_E(\omega_o)$ (in this case, $\sim$65 ns) is used in (29) to generate the plot.

As is concluded from the previous analysis, the in-band ripple of the combined filter equalizer network can be improved with higher ($\sim$>40 dB) isolation of the circulator. Since it is either difficult or very expensive to get such circulators at the desired frequency band, the hybrid-coupled approach [shown in Fig. 1(b)] seems attractive. A two-branch narrow-band 3-dB hybrid in the microstrip structure has been built. The measured response shows an isolation of better than 40 dB at the lower half of the band with around 35-dB isolation at the upper half. The 3-dB hybrid coupled network is constructed in the manner shown in Fig. 1(b) and the measured in-band responses are shown in Fig. 12. The simulated group-delay response is also included for comparison and good agreement is observed. The direct relationship between the isolation of the cascading device and the ripple of the final group-delay response is clearly observed in this figure.

V. Conclusion

A powerful and systematic method for the design of coupled-resonators group-delay equalizers has been introduced. This method consists of solving the approximation problem by optimization and synthesis of the network parameters. The presented method is insensitive to the initial guess of the locations of zeros and poles, and converges fast even when the number of cavities is large. Numerical considerations to both speed up the convergence of optimization and improve the accuracy have been discussed. Typical examples, together with experimental results of practical equalizers, have been presented. Extensive comparisons between the self-equalized and externally equalized structures have been made and the pros and cons have been summarized. The effect of the isolation of the cascading device on the ripple of the final group-delay response has been investigated. It is not feasible to compensate the effect of finite isolation of the cascading device (circulator or 3-dB hybrid) using the coupled-resonators structure. The effectiveness and powerful nature of the method have been proven by the good agreement between the simulation and measurement results.

References

[1] C. M. Kudsia, S. Kallianteris, and M. N. S. Swamy, "Linear phase versus externally equalized longitudinal dual-mode filters for space application," in *IEEE MTT-S Int. Microwave Symp. Dig.*, 1978, pp. 220–222.

[2] S. Kallianteris, "Low loss linear phase filters," in *IEEE MTT-S Int. Microwave Symp. Dig.*, June 1977, pp. 394–396.

[3] R. Levy, "Filters with single transmission zeros at real or imaginary frequencies," *IEEE Trans. Microwave Theory Tech.*, vol. MTT-24, pp. 172–181, Apr. 1976.

[4] C. M. Kudsia and V. O'Donovan, *Microwave Filters for Communications Systems*. Norwood, MA: Artech House, 1974.

[5] E. G. Cristal, "Theory and design of transmission line all-pass equalizers," *IEEE Trans. Microwave Theory Tech.*, vol. MTT-17, pp. 28–38, Jan. 1969.

[6] J. O. Scanlan and J. D. Rhodes, "Microwave all-pass network—Part I," *IEEE Trans. Microwave Theory Tech.*, vol. MTT-16, pp. 62–79, Feb. 1968.

[7] M. H. Chen, "The design of a multiple cavity equalizer," *IEEE Trans. Microwave Theory Tech.*, vol. MTT-30, pp. 1380–1383, Sept. 1982.

[8] A. E. Atia, A. E. Williams, and R. W. Newcomb, "Narrow-band multiple-coupled cavity synthesis," *IEEE Trans. Circuit Syst.*, vol. CAS-21, pp. 649–655, Sept. 1974.

[9] M. H. Chen, "Short-circuit tuning method for singly terminated filters," *IEEE Trans. Microwave Theory Tech.*, vol. MTT-25, pp. 1032–1036, Dec. 1977.

[10] A. E. Atia and H. W. Yao, "Coupling and resonant frequency measurements of cascaded resonators," in *IEEE MTT-S Int. Microwave Symp. Dig.*, June 2000, pp. 1637–1640.

[11] H. T. Hsu, H. W. Yao, K. A. Zaki, and A. E. Atia, "Design of coupled-resonator group delay equalizers," in *IEEE MTT-S Int. Microwave Symp. Dig.*, May 2001, pp. 1603–1606.

Heng-Tung Hsu (S'98) received the B.S. and M.S. degrees in electronics engineering from the National Chiao Tung University, Hsinchu, Taiwan, R.O.C., in 1993 and 1995, respectively, and is currently working toward the Ph.D. degree in electrical and computer engineering at the University of Maryland at College Park.

Hui-Wen Yao (S'92–M'95–SM'97) received the B.S. and M.S. degrees from the Beijing Institute of Technology, Beijing, China, in 1983 and 1986, respectively, and the Ph.D. degree from the University of Maryland at College Park in 1995, all in electrical engineering.

From 1986 to 1991, he was a Lecturer with the Department of Electrical Engineering, Beijing Institute of Technology, where his research dealt mainly with electromagnetic radiation, scattering, and antenna design. From 1992 to 1995, he was a Research Assistant in the Department of Electrical Engineering, University of Maryland at College Park, where he was involved with the analysis, modeling, and design of microwave and millimeter-wave devices and circuits. In 1995, he joined CTA Inc. Since 1997, he has been with the Orbital Sciences Corporation, Dulles, VA, where he is responsible for satellite communications systems. He has authored or co-authored 50 technical papers.

Dr. Yao is on the Editorial Board of the IEEE Transactions on Microwave Theory and Techniques. He was the recipient of the 1998 Outstanding Technical Achievement Award presented by the Orbital Sciences Corporation.

Kawthar A. Zaki (SM'85–F'91) received the B.S. degree (with honors) from Ain Shams University, Cairo, Egypt, in 1962, and the M.S. and Ph.D. degrees from the University of California at Berkeley, in 1966 and 1969, respectively, all in electrical engineering.

From 1962 to 1964, she was a Lecturer in the Department of Electrical Engineering, Ain Shams University. From 1965 to 1969, she was a Research Assistant in the Electronics Research Laboratory, University of California at Berkeley. In 1970, she joined the Electrical Engineering Department, University of Maryland at College Park, where she is currently a Professor of electrical engineering. Her research interests are in the areas of electromagnetics, microwave circuits, simulation, optimization, and computer-aided design of advanced microwave and millimeter-wave systems and devices. She has authored or co–authored over 200 publications. She holds five patents on filters and dielectric resonators.

Prof. Zaki was the recipient of several academic honors and awards for teaching, research, and inventions.

Ali E. Atia (S'67–M'69–SM'78–F'87) received the B.S. degree from Ain Shams University, Cairo, Egypt, in 1962, and the M.S. and Ph.D. degrees in electrical engineering from the University of California at Berkeley, in 1966 and 1969, respectively.

He is currently the President with the Space Systems Group, Orbital Sciences Corporation, Dulles, VA, where he is responsible for the communications business area, which builds communications and broadcasting satellites. In 1969, he joined COMSAT Laboratories, where he participated in research and development of a broad range of advanced microwave technologies for communication satellite transponders and antennas. He designed, developed, and implemented microwave flight hardware (mixers, filters, multiplexers, amplifiers, switches, antennas, etc.) for several satellite programs covering L- through the Ka- frequency bands. While with COMSAT Laboratories, he and his coworkers invented the dual-mode waveguide multiple coupled cavity filters, which has become the industry standard for input and output multiplexers in communication satellites, as well as other challenging filtering requirements. He has participated in and directed system development and software activities for several satellite programs and ground stations projects for customers including INTELSAT, INMARSAT, ARABSAT, and others. He has held several technical and management positions at COMSAT, the most recent of which was Vice President and Chief Engineer for the COMSAT Technology Services and COMSAT Systems Division. He has authored or co-authored over 100 refereed technical papers and presentations in IEEE publications and various national and international conferences and symposia. He holds five patents in the areas of microwave filters and receivers.

Dr. Atia is a Fellow of the American Institute of Aeronautics and Astronautics (AIAA). He is a member of Sigma Xi.